Journal of Minerals and Materials Characterization and Engineering, 2025, 13(1), 18-30
https://www.scirp.org/journal/jmmce
ISSN Online: 2327-4085
ISSN Print: 2327-4077

Evaluation of the Effectiveness of Traditional and Nano Materials Used in Consolidation of Sandstone Used in Ramesses III Temple, Karnak, Egypt

Essam H. Mohamed[1], Zeinab Mahmoud Ahmed[2], Mahmoud L. Abd El-Latif[3]

[1]Department of Archaeological Conservation, Faculty of Archaeology, South Valley University, Qena, Egypt
[2]Department of Conservation, Faculty of Archaeology, South Valley University, Qena, Egypt
[3]Housing and Building Research Center, Giza, Egypt
Email: essam.mohamed@arch.svu.edu.eg

How to cite this paper: Mohamed, E.H., Ahmed, M.Z. and El-Latif, M.L.A. (2025) Evaluation of the Effectiveness of Traditional and Nano Materials Used in Consolidation of Sandstone Used in Ramesses III Temple, Karnak, Egypt. *Journal of Minerals and Materials Characterization and Engineering*, **13**, 18-30.
https://doi.org/10.4236/jmmce.2025.131002

Received: March 6, 2023
Accepted: January 20, 2025
Published: January 23, 2025

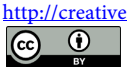

Abstract

This experimental study assesses the effectiveness of traditional and nano-materials in enhancing the physical and mechanical properties of deteriorated sandstone from Ramesses III Temple, Karnak, Luxor, Egypt. Treatments included Nano Estel (5%), Paraloid B-72 (3%), Paraloid B-72/Nano Estel (3%/5%), and ethyl silicates. Treated samples underwent Scanning Electron Microscopy (SEM) and physical/mechanical testing. Results show that Paraloid B-72/Nano Estel (3%/5%) yielded optimal consolidation, significantly improving sandstone's physical and mechanical properties.

Keywords

Ramesses III Temple, Deteriorated Sandstone, Consolidation Treatments, Nano Material, Physical and Mechanical Properties

1. Introduction

Cultural heritage conservation is vital, as historical buildings provide irreplaceable insights into architectural innovation and societal development. This research explores the prominence of sandstone in ancient Egyptian construction and artistry, examining its role in iconic temples and sculptures, and highlighting its cultural significance [1]. Ancient Egyptian temples were constructed from sandstone, a sedimentary rock prone to weathering, face degradation due to high porosity and moisture exposure [2]. Salt crystallization beneath the surface of porous stone causes structural pressure, leading to cracking due to hydration-dehydration cycles

[3]. This study explores how geological background affects sandstone characteristics, focusing on predictive relationships between mineralogical properties and uniaxial compressive strength [4]. Iron compound oxidation in stone leads to color alteration and structural degradation.

The clay-rich cementing phase in sandstones predisposes them to degradation through moisture-driven expansion/contraction and salt-mediated stress [5] [6]. Deterioration symptoms through granular disintegration, exfoliation, detachment, cracking, efflorescence, discoloration, and microbiological colonization [7]. Paraloid B72's suitability for stone conservation is substantiated by numerous studies demonstrating its adhesive and consolidate properties [8]. Studies confirm Paraloid B72's efficacy, providing comprehensive pore filling (90%) and particle coverage, enhancing sandstone durability [9]. Ethyl silicate consolidants, producing colloidal silica, offer excellent compatibility with silicate-based stones like sandstone [10]. Nano Estel restores stone cohesion via nano silica's siloxane bond (Si-O-Si) formation through hydrolysis, condensation, and polymerization. Hydrolysis-induced silanol formation and subsequent condensation polymerization facilitate nano silica-mediated stone consolidation [11]. Recent research confirms improved consolidation efficiency and strength of ancient building materials using nano silica and nano titanium [12]. This study explores Nano composite applications in consolidation of sandstone, demonstrating improved physical, chemical, and mechanical properties, and enhanced durability for stone monuments [13], comparative evaluation of treated sandstone samples reveals enhanced consolidation and protection via nanoparticle-acrylic polymer composites, nanoparticle-infused polymers demonstrate improved efficiency in sandstone consolidation and preservation.

2. Ramsses III Temple

The Temple of Ramses III, situated within the Karnak temple complex in Luxor, showcases ancient Egyptian architecture's grandeur (**Figure 1**, **Figure 2**) [12]. Sandstone degradation accelerates in harsh environments, characterized by temperature fluctuations, moisture and pollution, environmental factors, including temperature swings and moisture, exacerbate sandstone deterioration, thermal expansion-induced cracking threatens sandstone integrity in fluctuating environmental conditions.

Chemical characteristics, including solubility, corrosion resistance, and weathering resistance, are intimately linked with physical properties such as density, porosity, and hardness. A strong correlation exists between chemical qualities (solubility, corrosion resistance, weathering resistance) and physical attributes (density, porosity, hardness) of materials [13]. Sandstones predominantly comprise quartz, a resilient detrital mineral characterized by its strong silicon-oxygen bonds, resistance to chemical weathering, and absence of cleavage [14]. Sandstone weathering durability is closely tied to pore space characteristics, including porosity, permeability, and pore geometry, especially in clay-dominated matrices/pseudo matrices [15].

Figure 1. The first hypostyle hall of Ramesses III Temple.

Figure 2. Location of Karnak in Egypt (https://www.britannica.com/place/Karnak).

Field Observations and Deterioration Causes

Ramesses III temple walls exhibit pronounced deterioration, particularly in lower sections, due to fluctuating temperature and relative humidity. Repeated expansion and contraction of mineral granules induce internal stresses, leading to cracking [16]. The Temple of Ramses III's proximity to the Nile River, coupled with its elevated position (2 m above surrounding land), exposes sandstone structures to heightened moisture levels from subsurface water, exacerbating deterioration. Groundwater infiltration into the Temple of Ramses III's foundations, facilitated by capillary action, introduces salts detrimental to stone blocks. Temperature and humidity fluctuations exacerbate sandstone degradation through mineral grain disintegration [17]. The Temple of Ramses III's sandstone surfaces undergo physical, chemical, and mechanical deterioration due to plant root growth, bird droppings, and bacterial activity. Soluble salts in avian excrement exacerbate degradation (**Figure 3**) [18].

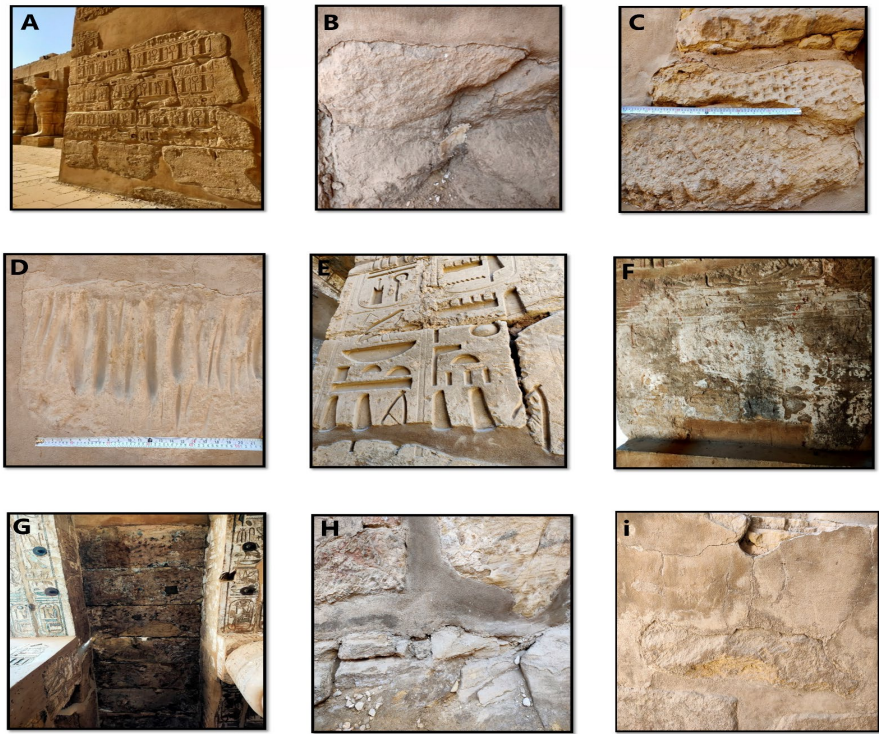

Figure 3. Different deterioration symptoms of Ramesses III temple (A) macro-cracks spread on the surfaces. (B) Black weathering due to Loss of scales. (C) alveolar weathering due to lose of stone material. (D) Relief. (E) Break out due to natural cause. (F) Efflorescences to light-colored crust changing the surface. (G) Microbiological colonization to dark-colored crust tracing the surface. (H) Granular disintegration into powder. (i) weathering out dependent on stone structure.

3. Materials and Methods

3.1. Materials

3.1.1. Preparation of Sandstone Samples

Sandstone samples from Jabal Al-Silsilah quarries (**Figure 4**) were precision-cut into 3 × 3 × 3 cm cubes, oven-dried (65˚C, 24 h) and cooled (RH 50%) according to ASTM standards, ensuring constant weight for treatment testing.

Figure 4. The prepared representative samples.

3.1.2. Consolidation Materials

- Paraloid B-72

Paraloid B-72, a 70/30 ethyl methacrylate (EMA) and methyl acrylate (MA) copolymer, was prepared as a 3% (w/v) solution in toluene.

- Ethyl Silicate

SILRES BS OH 100, an ethyl silicate-based consolidate, penetrates construction materials via capillary action, forming a durable SiO_2 gel binder upon reaction with atmospheric humidity or moisture. The treated area should be protected against rain during the following two to three days. It is also important that the area be protected against direct sunlight prior to treatment. If the building material is allowed to absorb too much heat, the product will evaporate too quickly and therefore will not penetrate sufficiently. The optimum temperatures for application are between 10˚C and 20˚C. The relative humidity should be >40%.

- Nano Estel

Nano Estel, a colloidal nano-silica dispersion (10 - 20 nm), exhibits enhanced penetrability and stability due to sodium hydroxide (NaOH < 0.5%) stabilization, demonstrating an alkaline pH (9.8 - 10.4).

Because of the water evaporation, the particles bind among themselves forming a silica gel, similarly to what happens for ethyl silicate, and thus determining the consolidating effect. Nano Estel's Nano-silica particles undergo evaporative-induced aggregation, forming a three-dimensional silica gel network, thereby enhancing material cohesion.

- Nano Estel+ Paraloid B-72

A nanocomposite consolidant was synthesized by dispersing 3% silica nanoparticles within Paraloid B-72/trichloroethylene solutions, as shown Table 1.

Table 1. The consolidation materials and Sample's number.

Samples code	Consolidation Materials	
1 - 6	Nano Estel	5%
7 - 12	Paraloid B-72	3%
13 - 18	Nano Estel + B-72	3% - 5%
19 - 24	Ethyl Silicate	5%

3.2. Methods

3.2.1. Examinations

The mineralogical composition of sandstone samples was investigated using transmitted polarized light microscopy (Olympus BX50) and X-ray diffraction (Pert Pro Phillips MPD PW 3050/60) at HBRC laboratories, Dokki, Giza, Egypt. Scanning Electron Microscopy (SEM) investigation was performed on deteriorated sandstone samples using a JEOL JSM-5500 LV (JEOL, Japan) at laboratories of South valley university. Scanning Electron Microscopy (SEM) investigation aimed to assess consolidation material penetration and distribution within sandstone grains and components, evaluating consolidation efficacy.

3.2.2. Physical and Mechanical Properties of the Samples

The impact of consolidation materials on physical and mechanical properties of sandstone samples were assessed through quantitative measurements.

1) Visual examination

Post-consolidation, sandstone samples exhibited varying degrees of visual change, dependent on treatment material.

2) Physical Properties

Physical properties (density, water absorption, and porosity) of untreated and treated sandstone samples were evaluated using standard test methods [19] [20].

3) Mechanical Properties

Compressive strength values of untreated and consolidated sandstone samples were determined following [standard/test method, e.g., ASTM C109] [21]-[23].

4. Consolidation Process

Consolidation treatments were applied to 24 sandstone samples, divided into four groups: Nano Estel (A), Paraloid B72 (B), Paraloid B72/Nano Estel (C), and ethyl silicate (D).

Treatment materials' suitability for consolidation of sandstone were assessed through immersion testing to ensure safe and effective application, Sandstone samples underwent 21-day consolidation treatment via immersion in respective materials, allowing complete polymerization, as shown **Figure 5**.

Figure 5. The sandstone samples after consolidation.

5. Results and Discussion

5.1. Mineralogical and Textural Composition

Petrographic examination indicated the quartz arenite sandstone sample is characterized by quartz grains (95%) cemented by micritic carbonate and featuring localized iron oxide coatings, and also, thin orange and brown coating at edges of some quartz grains which due to presence of iron content as shown in (**Figure 6**). On the other hand, XRD showed a complete agreement with polarizing microscope as quartz represents the primary mineral in studied sandstone forming minerals associated with traces of feldspar (albite) as detected in XRD pattern (**Figure 7**).

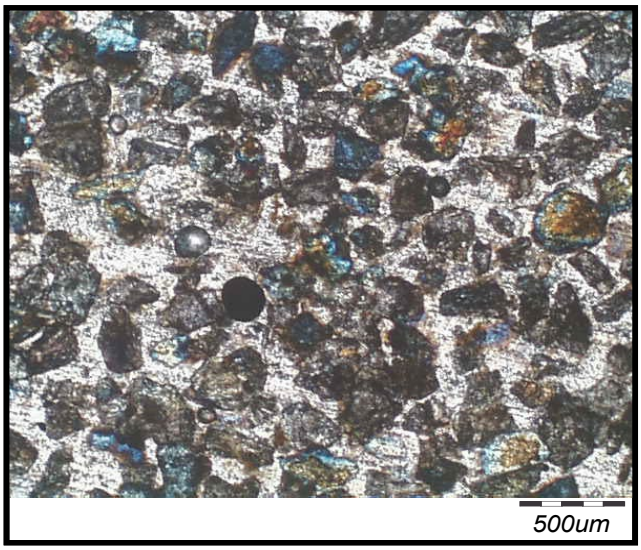

Figure 6. Photograph of the deteriorated sandstone.

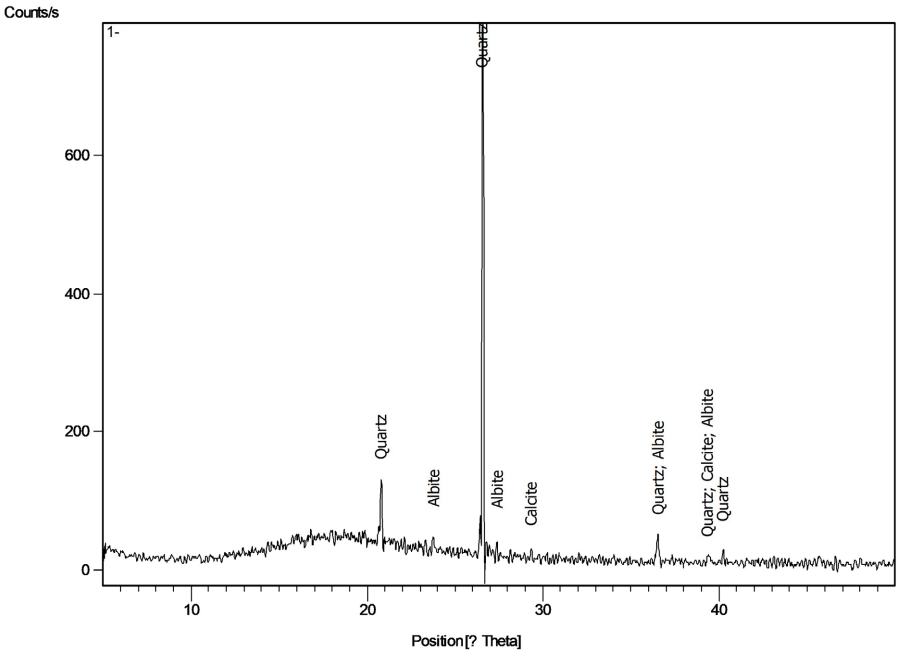

Figure 7. XRD pattern of the deteriorated sandstone.

5.2. SEM Results

Scanning Electron Microscopy (SEM) facilitated characterization of consolidation material properties and sandstone interaction, illustrating treatment efficacy, the samples were shown in (**Figure 8**). Consolidation treatments yielded varying degrees of success, visible through SEM micrographs that show different consolidation effects:

1) Nano Estel: Deep penetration and dense packing.
2) Paraloid B-72: Good penetration and pour filling.
3) Nano Estel + B-72: Enhanced coating and filling.

4) Ethyl Silicate: Uniform diffusion.

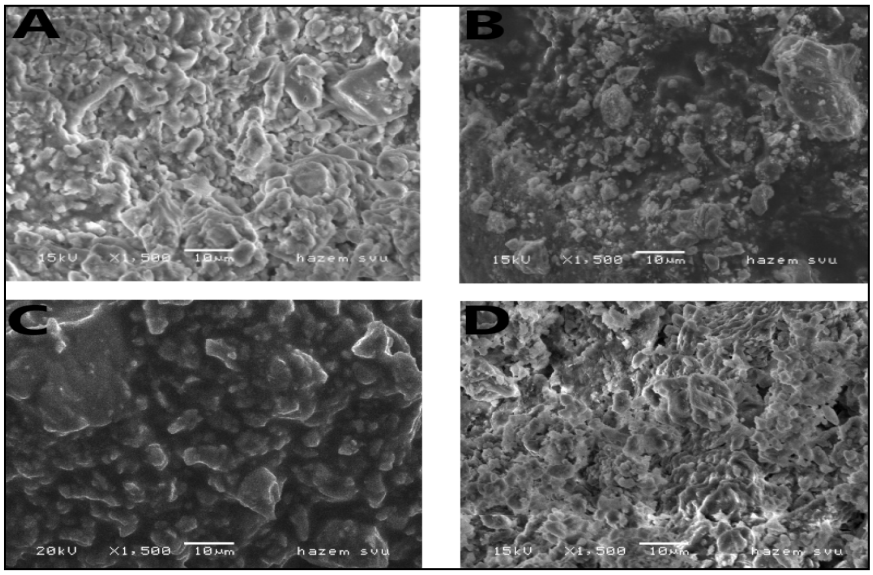

Figure 8. SEM micrographs of the treated sandstone samples. (A) The SEM examination of the treated samples with Nano Estel (1.500X). (B) The examination of the treated samples with Paraloid B-72 (1.500X). (C) The SEM examination of the treated samples with Nano Estel+B-72 (1.500X). (D) The examination of the treated samples with Ethyl Silicate (1.500X).

5.3. Physical Properties of the Treated Samples

Consolidation material success hinges on minimal visual impact, specifically no discernible color or appearance alteration of the building materials, Visual inspection of treated samples provides preliminary assessment of treatment efficacy, subsequent testing follows visual evaluation, with materials exhibiting noticeable appearance changes being disqualified, it is excluded even if this material proves to be successful in the other tests. Treated sandstone samples underwent visual inspection and comparison to untreated controls to determine consolidation effectiveness, Visual evaluation ranked consolidation materials by transparency: Nano Estel (1st), Paraloid B72/Nano Estel (2nd), Paraloid B72 (3rd), and Ethyl Silicate (4th) (Table 2).

Table 2. Visual examination of the consolidated samples.

Samples cod	Consolidation Material	Effect of appearance
A	Nano Estel	No Surface changes
B	Paraloid B-72	slight color change
C	Nano Estel + B-72	slight color change
D	Ethyl Silicate	Noticeable color change

Water repellency testing ranked consolidation materials: Paraloid B72 (1st), Paraloid B72/Nano Estel (2nd), Ethyl Silicate (3rd), and Nano Estel (4th) (Figure 9).

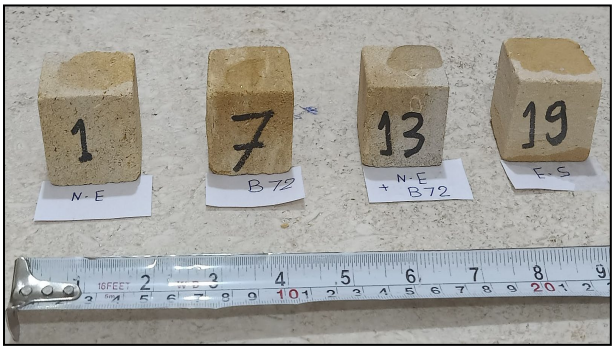

Figure 9. Water Repellents of the treated samples after consolidation.

The Paraloid B72/Nano Estel mixture yielded a porosity rate of 6.71%, representing a 55.53% reduction compared to the untreated sample (15.09%); Paraloid B-72 treatment yielded a porosity rate of 8.67%, representing a 42.54% reduction from the untreated sample (15.09%); Nano Estel-treated samples exhibited a porosity rate of 9.72%, showing a 35.58% reduction. Ethyl Silicate-treated samples ranked lowest, Ethyl Silicate-treated samples exhibited the highest porosity rate (10.72%), representing a 29.68% reduction from the untreated sample (15.09%) (**Table 3**, **Figure 10**).

Table 3. The means values of the physical properties of the treated samples.

Samples code	Consolidation Material	Porosity %	Density g/cm³	Water absorption %
X	Untreated Sample	15.09	2.17	27.2
A	Nano Estel	9.72	2.25	17.16
B	Paraloid B-72	8.67	2.30	15.63
C	Nano Estel + B-72	6.71	2.35	12.11
D	Ethyl Silicate	10.61	2.20	19.14

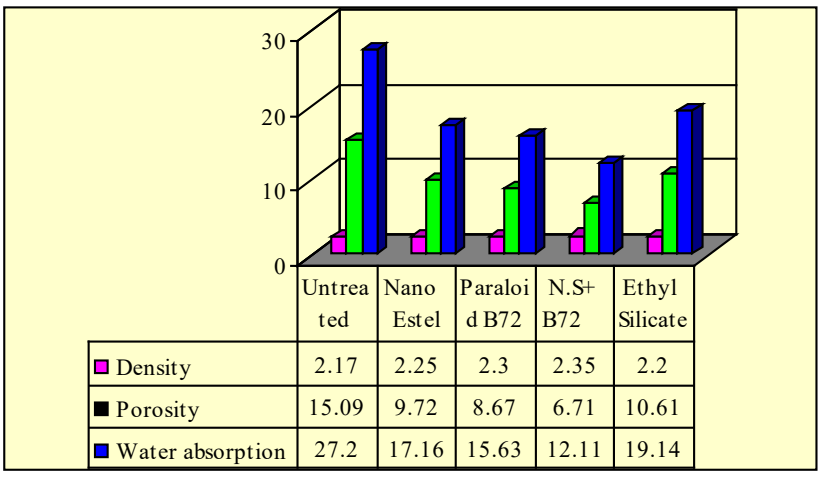

Figure 10. The mean values of physical properties after treatments.

The Nano Estel + Paraloid B-72 mixture exhibited the lowest water absorption rate (12.11%), representing a 55.47% reduction compared to the untreated sample

(27.2%), Paraloid B-72-treated samples exhibited an average water absorption rate of 15.63%, representing a 43.53% reduction compared to the standard sample, Nano Estel-treated samples showed 17.16% water absorption, a 36.91% reduction. Ethyl silicate-treated samples exhibited 19.14% absorption, a 29.63% decrease (Table 3, Figure 10).

Density measurements were conducted to assess the efficacy of various consolidating materials. The results indicated a significant increase in density values for treated samples, with Paraloid B72/Nano Estel-treated samples achieving an average density of 2.35 g/cm^3, representing an 82.94% increase compared to untreated samples, which recorded 2.17 g/cm^3. Subsequently, Paraloid B-72-treated samples exhibited a mean density of 2.30 g/cm^3, representing an 59.90% increase compared to untreated samples. Nano Estel-treated samples exhibited a mean density of 2.25 g/cm^3, representing a 36.86% increase. The average density of ethyl silicate-treated samples was 2.20 g/cm^3, with an 18.43% enhancement (Table 3, Figure 10).

5.4. Mechanical Properties

The Paraloid B-72/Nano Estel-treated samples achieved the highest compressive strength value of 232 kg/cm^2, compared to 170 kg/cm^2 for the untreated sample. The compressive strength of Paraloid B-72-treated samples reached 218 kg/cm^2, exceeding the untreated sample. The compressive strength of Nano Estel-treated samples reached 192 kg/cm^2. Finally, samples treated with ethyl silicate showed a compressive strength of 188 kg/cm^2 (Table 4) (see Figure 11).

Table 4. The means values of mechanical properties of the treated samples.

Samples code	Consolidation Materials	Compressive strength (Kg/cm^2)
X	Untreated Sample	170
A	Nano Estel	192
B	Paraloid B72	218
C	Nano ESTEL + B72	232
D	Ethyl Silicate	188

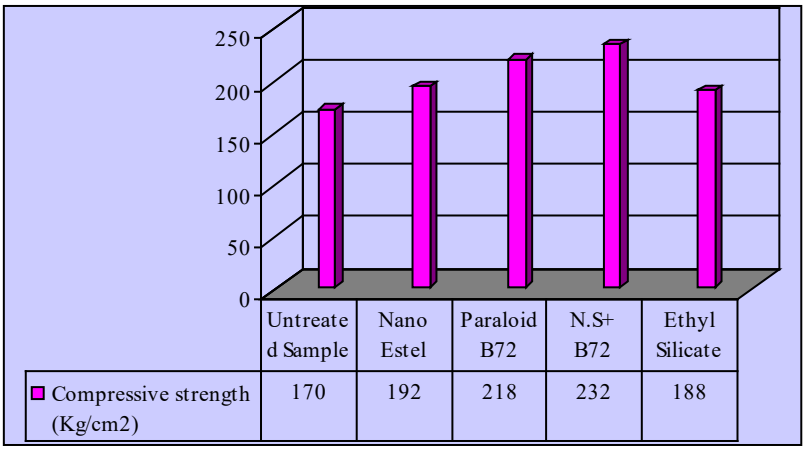

Figure 11. The mean values compressive strength of the treated samples.

6. Conclusions and Recommendations

Dependence on the obtained results among the recent study, it can be concluded that:

1) The selection of consolidation materials for the studied sandstone required materials closely resembled to its physical, mineralogical, and chemical characteristics.

2) Four consolidation materials were chosen carefully to achieve the aim of the recent study. Two of them were classified as traditional involving Paraloid B72 and Ethyl Silicate while others were classified as nano consolidated materials involving Nano Estel and Nano Estel added Paraloid B72.

3) The positive effect of consolidation materials can be appeared from the regression in the water absorption and porosity for treated samples compared to untreated sample associated with increase in values of bulk density and compressive strength for treated samples in compare with untreated samples.

4) The most promising obtained results achieved by treated sandstone samples with 5% nano estel particles with 3% Paraloid B_72 compared to individually treated with nanomaterials.

Finally, it can be recommended that Nano Estel + B72 the most suitable consolidation materials for the studied sandstone.

Conflicts of Interest

The authors declare no conflicts of interest regarding the publication of this paper.

References

[1] Siegesmund, S., Weiss, T. and Vollbrecht, A. (2002) Natural Stone, Weathering Phenomena, Conservation Strategies and Case Studies: Introduction. *Geological Society, London, Special Publications*, **205**, 1-7. https://doi.org/10.1144/gsl.sp.2002.205.01.01

[2] Fitzner, B., Heinrichs, K. and Bouchardiere, D.L. (2003) Weathering Damage on Pharaonic Sandstone Monuments in Luxor-Egypt. *Building and Environment*, **38**, 1089-1103. https://doi.org/10.1016/s0360-1323(03)00086-6

[3] Ruedrich, J., Bartelsen, T., Dohrmann, R. and Siegesmund, S. (2010) Moisture Expansion as a Deterioration Factor for Sandstone Used in Buildings. *Environmental Earth Sciences*, **63**, 1545-1564. https://doi.org/10.1007/s12665-010-0767-0.

[4] Harrell, J.A. (2016) Varieties and Sources of Sandstone Used in Ancient Egyptian Temples. *Journal of Ancient Egyptian Architecture*, **1**, 11-37.

[5] Götze, J. and Siedel, H. (2004) Microscopic Scale Characterization of Ancient Building Sandstones from Saxony (germany). *Materials Characterization*, **53**, 209-222. https://doi.org/10.1016/j.matchar.2004.08.016

[6] Mohamed, E.H. (2022) Study Correlation between Physical-Mineralogical Properties of Sandstone Used in Ptolemaic Temples in Upper Egypt and Its Weathering Resistance. *Journal of Minerals and Materials Characterization and Engineering*, **10**, 371-384. https://doi.org/10.4236/jmmce.2022.105026

[7] Benavente, D., Cueto, N., Martínez-Martínez, J., García del Cura, M.A. and Cañaveras, J.C. (2006) The Influence of Petrophysical Properties on the Salt Weathering

of Porous Building Rocks. *Environmental Geology*, **52**, 215-224. https://doi.org/10.1007/s00254-006-0475-y

[8] Mohamed, E.H. (2023) Effectiveness Assessment of Paraloid B-72 Enhanced with Nano Materials to Improve of Completion Mortars Properties for Conservation of Seti I Temple in El-Qurna, Thebes West Bank, Egypt. *Multiscale and Multidisciplinary Modeling, Experiments and Design*, **6**, 371-387. https://doi.org/10.1007/s41939-023-00152-1

[9] Labus, M. and Bochen, J. (2012) Sandstone Degradation: An Experimental Study of Accelerated Weathering. *Environmental Earth Sciences*, **67**, 2027-2042. https://doi.org/10.1007/s12665-012-1642-y

[10] Schaffer, R.J. (2016) The Weathering of Natural Building Stones. Routledge. https://doi.org/10.4324/9781315793771

[11] Deprez, M., De Kock, T., De Schutter, G. and Cnudde, V. (2020) A Review on Freeze-Thaw Action and Weathering of Rocks. *Earth-Science Reviews*, **203**, 103143. https://doi.org/10.1016/j.earscirev.2020.103143

[12] Alexandrowicz, Z., Marszałek, M. and Rzepa, G. (2013) Distribution of Secondary Minerals in Crusts Developed on Sandstone Exposures. *Earth Surface Processes and Landforms*, **39**, 320-335. https://doi.org/10.1002/esp.3449.

[13] Adamovic, J., Mikulas, R., Schweigstillova, J. and Bohmova, V. (2011) Porosity Changes Induced by Salt Weathering of Sandstones, Bohemian Cretaceous Basin, Czech Republic. *Acta Geodynamica et Geromaterialia*, **8**, 29-46.

[14] Ameratunga, J., Sivakugan, N. and Das, B.M. (2016) Correlations of Soil and Rock Properties in Geotechnical Engineering. https://doi.org/10.1007/978-81-322-2629-1

[15] Hossam, I. (2015) The Climate and Its Impacts on Egyptian Civilized Heritage: Ei-Nadura Temple in El-Kharga Oasis, Western Desert of Egypt as a Case Study. *Present Environment and Sustainable Development*, **9**, 5-32. https://doi.org/10.1515/pesd-2015-0001

[16] El-Gohary, M.A. (2017) Environmental Impacts: Weathering Factors, Mechanism and Forms Affected the Stone Decaying in Petra. *Journal of African Earth Sciences*, **135**, 204-212. https://doi.org/10.1016/j.jafrearsci.2017.08.020

[17] Mohamed, E.H. (2020) Assessment of the Current State of Qanibay Al-Rammah Complex (908 AH/1502 AD), as a Procedure Precedes the Restoration Process. *Open Journal of Geology*, **10**, 71-91. https://doi.org/10.4236/ojg.2020.101004

[18] Radwan, A.E., Wood, D.A., Abudeif, A.M., Attia, M.M., Mahmoud, M., Kassem, A.A., *et al.* (2021) Reservoir Formation Damage; Reasons and Mitigation: A Case Study of the Cambrian-Ordovician Nubian 'C' Sandstone Gas and Oil Reservoir from the Gulf of Suez Rift Basin. *Arabian Journal for Science and Engineering*, **47**, 11279-11296. https://doi.org/10.1007/s13369-021-06005-8

[19] Sebastián, E., Cultrone, G., Benavente, D., Linares Fernandez, L., Elert, K. and Rodriguez-Navarro, C. (2008) Swelling Damage in Clay-Rich Sandstones Used in the Church of San Mateo in Tarifa (Spain). *Journal of Cultural Heritage*, **9**, 66-76. https://doi.org/10.1016/j.culher.2007.09.002

[20] ASTM C-97 (2018) Standard Test Methods for Absorption and Bulk Specific Gravity of Dimension Stone. https://www.astm.org/c0097_c0097m-18.html

[21] ASTM C20-00 (2015) Standard Test Methods for Apparent Porosity, Water Absorption, Apparent Specific Gravity and Bulk Density of Burned Refractory Brick and Shapes by Boiling Water. Annual Book of ASTM Standards, 15.01. https://www.scirp.org/reference/referencespapers?referenceid=2328149

[22] ASTM C-170 (2015) Standard Test Method for Compressive Strength of Dimension Stone.

[23] Wüst, R.A.J. and McLane, J. (2000) Rock Deterioration in the Royal Tomb of Seti I, Valley of the Kings, Luxor, Egypt. *Engineering Geology*, **58**, 163-190. https://doi.org/10.1016/s0013-7952(00)00057-0